Optimal Power Scheduling and Techno-Economic Analysis of a Residential Microgrid for a Remotely Located Area: A Case Study for the Sahara Desert of Niger

Issoufou Tahirou Halidou [1,*], Harun Or Rashid Howlader [2,*], Mahmoud M. Gamil [1,3], M. H. Elkholy [1,3] and Tomonobu Senjyu [1]

1   Graduate School of Engineering and Science, University of the Ryukyus, 1 Senbaru, Nakagami-Gun, Nishihara-Cho, Okinawa 903-0213, Japan; k228677@cs.u-ryukyu.ac.jp (M.H.E.)
2   Hawai'i Natural Energy Institute, University of Hawai'i at Manoa, Honolulu, HI 96822, USA
3   Department of Electrical Power and Machines, Faculty of Engineering, Zagazig University, Zagazig 44519, Egypt
*   Correspondence: thissoufou@gmail.com (I.T.H.); harun@hawaii.edu (H.O.R.H.)

Abstract: The growing demand for electricity and the reconstruction of poor areas in Africa require an effective and reliable energy supply system. The construction of reliable, clean, and inexpensive microgrids, whether isolated or connected to the main grid, has great importance in solving energy supply problems in remote desert areas. It is a complex interaction between the level of reliability, economical operation, and reduced emissions. This paper investigates the establishment of an efficient and cost-effective microgrid in a remote area located in the Djado Plateau, which lies in the Sahara Ténéré desert in northeastern Niger. Three cases are presented and compared to find the best one in terms of low costs. In case 1, the residential area is supplied by PVs and a battery energy storage system (BESS), while in the second case, PVs, a BESS, and a diesel generator (DG) are utilized to supply the load. In the third case, the grid will take on load-feeding responsibilities alongside PVs, a BESS, and a DG (used only in scenario 1 during the 2 h grid outage). The central objective is to lower the cost of the proposed microgrid. Among the three cases, case 3, scenario 2 has the lowest LCC, but implementing it is difficult because of the nature of the site. The results show that case 2 is the best in terms of total life cycle cost (LCC) and no grid dependency, as the annual total LCC reaches about $2,362,997. In this second case, the LCC is 11.19% lower compared to the first case and 5.664% lower compared to the third case, scenario 1.

Keywords: microgrid; mixed-integer linear programming (MILP); power scheduling; optimal sizing; grid outage

1. Introduction

1.1. Motivations

Using the World Bank Development Indicators, it has been shown that the use of energy is strongly related to almost every conceivable aspect of development. Wealth, health, nutrition, water, infrastructure, education, and even life expectancy itself, are strongly and significantly related to the consumption of energy per capita [1]. That is to say that energy is vital for all living beings on Earth. Its availability is one of the basic conditions for the sustainable development and social well-being of any nation. However, this sustainable development is far from being achieved, especially for developing countries, as a result of an energy demand that grows exponentially due to population growth. Hence, the number of people living in energy poverty, referred to here to as non-access to electricity, is estimated to be around 1.2 billion (16% of the world's population), and a large number of these people are from Sub-Saharan Africa.

For the majority of their energy needs, many countries rely on fossil fuels (coal, gas, oil, uranium, etc). These conventional power sources have been the major methods of producing electricity. According to [2–5], 85% of the global energy supply comes from conventional power sources. However, reliance on these fuels presents a challenge for the future as they tend towards depletion and they also present serious threats to human lives. In addition, supplying electricity to rural communities is not an easy task due to economic and geographical issues. These isolated communities frequently rely on diesel generators to obtain electricity. The cost of running these diesel generators and the huge environmental pollution are not favorable [6–8]. To overcome the aforementioned problems, renewable energy resources have drawn the attention of researchers to face the depletion of fossil fuels, to prevent global warming, and especially to electrify off-grid communities or to provide a constant electricity supply. In contrast to conventional energy sources, renewable energy sources are inexhaustible and lasting energy sources. They are available in all countries, and their potential is yet to be fully harnessed. According to the International Renewable Energy Agency (IRENA), about 90 percent of the world's electricity can and should come from renewable energy by 2050 [9]. The world needs renewable, reliable, sustainable, affordable, and modern energy resources for humanity because they are much cleaner, more cost effective, and produce energy without harming the environment. There are various renewable energy generation sources, such as hydropower, solar photovoltaics (PVs), wind turbines (WTs), biomass energy, geothermal energy, etc. In addition to their advantages, such as being environmental friendly and sustainable, PV energy and wind energy have been used frequently due to the reduction in their manufacturing cost and growing industrial and residential applications [10]. These sources can be connected individually as a hybrid to supply power to the grid [11,12]. Further, renewable energy sources can be used to electrify remote areas, which cannot be supplied from an accessible grid. However, these renewable energy sources generate significant disturbances due to their intermittent nature. Moreover, as a result of the non-reliability and excessive sizing of using a single source like PVs, to supply power to remotely located populations, hybrid renewable energy resources are proposed to meet these challenges [13]. Hybrid renewable energy systems (HRES) usually comprise one or more renewable sources (e.g., PVs, WTs, etc.), conventional diesel generators, and sometimes storage systems (e.g., batteries, pumped thermal storage systems, pumped hydro-energy storage systems, fuel cells, etc.). Storage systems play a vital role in the microgrid structure. Therefore, they can be used to supplement the power output variation of renewable sources that work totally erratically.

When configuring a hybrid system, the integrated sources must be appropriate to the nature of the region, its weather, and climatic conditions. Each renewable energy source has a different nature, so integrated systems must complement each other. Several studies have been conducted discussing the uncertainty and global sensitivity analysis of the output of RESs [14]. Many studies have been conducted to explore the integration of renewable energy sources to form an ideal hybrid system for supplying isolated microgrids or for connection to the main grid. Among the proposed configurations is the combination of wave, solar, and wind energies [15,16]. A recent study was conducted proposing a hybrid system that combines wave, solar, and wind energies [17]. Another approach is focused on improving the quality of renewable energy sources through the use of artificial intelligence [18,19]. A study was conducted to investigate hybrid renewable energy systems and ways to develop them through artificial intelligence [20]. Therefore, in this study, a set of configurations was studied to determine an optimal hybrid system that is suitable for the region's nature. Optimization techniques were used to achieve the most efficient and cost-effective microgrid in a remote desert area in the Djado Plateau in northeastern Niger.

1.2. Related Works

Recently, the use of hybrid photovoltaic (PV) and wind energy systems has been growing for off-grid applications. Several studies have been carried out on microgrid

schemes operating in standalone mode to build a green climate in line with the cost reduction of conventional diesel generators, and to electrify remote areas that cannot be supplied from an attainable utility grid. The authors of [21] showed that PV–biomass or PV–diesel hybrid systems provide ultimate reliability and the lowest cost for standalone electricity. The objective to satisfy consumers by generating continuous power using solar and wind systems at minimum cost was achieved in [22]. A cost–benefit study on a hybrid renewable energy system was optimized to electrify a rural Ethiopian village in [23]. Compared to a diesel-only system, a hybrid PV-wind-diesel-battery system was found to be the most cost-effective and had the lowest CO_2 emissions. According to [24], a hybrid photovoltaic/biomass/wind/pump-hydro scheme would be ideal for remote village, local hospital, education, and industrial sites.

Extending the use of HRES to electrify rural off-grid/on-grid locations has motivated researchers to examine more technical and economic feasibility problems. In [25,26], a techno-economic analysis was applied using the HOMER Pro software tool. In [25], a study was carried using the HOMER Pro software tool to redesign and refinance a remote HRES (diesel, PVs, and batteries) on a small island in Thailand. The HRES was optimized to reach the lowest cost of electricity. In [26], a study was developed to investigate the electrification of a rural community in Benin. The findings of this study revealed that the hybrid PV–diesel–battery system achieved the lowest-cost optimal system. However, the planning and optimal design of an HRES from an economic and technical point of view are challenging for various reasons. One is the inconsistency of renewable energy sources and their reliance on weather conditions. HRES systems are often either oversized or undersized to satisfy the energy demand. An oversized system will result in high system costs, generating surplus energy. Moreover, an undersized system will result in failure of the power supply to the targeted loads. To overcome the problems mentioned above and to fully utilize the benefit of the renewable-energy-based microgrid, optimal sizing of an HRES must be considered.

In recent times, great attention has been centered on studying the optimal sizing of an HRES. According to [27], GA was used to find the optimal sizing of an integrated hybrid PV–WT–battery system in an energy management strategy. Ref. [28] introduced a control methodology for controlling the microgrid using FPGA. The authors of [29] presented an improved fruit-fly optimizer technique to optimally design a hybrid PV–WT–diesel–battery system based on total annual cost (TAC) and pollutant emission minimization. The HOMER software tool was used to optimally size standalone hybrid systems in [30–33]. The authors of [34] studied various configurations in respect of microgrid system design using HOMER. In their article, different scenarios were compared in terms of the levelized cost of energy. In [35], the HOMER software tool was utilized to investigate electricity generation for a standalone system in Bangladesh. The capacity cost, net present cost, levelized energy cost, and wind power production of different hybrid system configurations were examined. The grasshopper optimization algorithm (GOA) was used in [36] to perform the optimal sizing of a hybrid autonomous microgrid for five residential units in an off-grid location in Yobe State, Nigeria. In their paper, the authors described the superiority of the GOA over particle swarm optimization (PSO) and cuckoo search (CS) in terms of fulfilling the demand of the residential housing reliably based on the deficiency of power supply probability (DPSP) and with a low cost of energy (COE).

The authors of [37] evaluated the performance of seven (7) different evolutionary algorithms for the optimum sizing of a PV/WT/battery hybrid system to continuously satisfy the load demand with the minimal total annual cost. They demonstrated that artificial bee swarm optimization (ABSO) gives more acceptable results than particle swarm optimization (PSO), tabu search (TS), simulated annealing (SA), improved particle swarm optimization (IPSO), improved harmony search (IHS), and improved-harmony-search-based simulated annealing (IHSBSA) in terms of TAC. By considering a maximum allowable loss of power supply probability ($LPSP_{max}$) set to 5%, the PV/battery is the most cost-effective hybrid system. Multiple objectives, including minimization of the life-cycle

cost, maximization of the renewable energy source penetration, and the minimization of pollutant emissions for solving the sizing optimization problem, combined with the operational strategy and operational experience of a real microgrid system on Dongfushan Island, Zhejiang Province, China, were employed for the GA-based method in [38].

In [39], the whale optimization algorithm (WOA), water cycle algorithm (WCA), moth-flame optimizer (MFO), and hybrid particle swarm-gravitational search algorithm (PSOGSA) were applied for the optimal design of a PV/wind/diesel/battery storage grid-independent hybrid microgrid for minimizing the COE while maximizing the reliability and the efficiency of the system presented by the loss of power supply probability. The optimization results revealed that the WOA proved its superiority in solving the optimization problem in terms of convergence, speed, and accuracy. The authors of [40] evaluated five scenarios to determine the best possible optimal HRES in terms of minimum net present cost (NPC), COE, and CO_2 emissions for Kutubdia Island in Bangladesh. A comprehensive comparison between the non-dominated sorting genetic algorithm (NSGA)-II-based optimization and hybrid optimization of multiple energy resources (HOMER) Pro software was presented; the NSGA-II-based optimization gave USD 692,775 as the NPC, which was less than that of the HOMER-based optimization (USD 711,943), for the best scenario, i.e., a PV/Wind/Battery/DG system.

In [41], a study was conducted to discuss the design and implementation of a hybrid system to electrify Dera Ismail Khan, a rural area located in Pakistan, combining PVs, a DG, and a BESS. Different scenarios were studied, whether connected or isolated from the national grid. That study concluded that the best solution was a hybrid system that combined PVs, a BESS, and a DG with a national grid. HOMER Pro was relied upon in the implementation of the study. A brief review of the recent developments in hybrid renewable energy systems that depend on optimization techniques was provided in [42]. The review discussed classical methods in addition to techniques that depend on artificial intelligence. It concluded that technologies that rely on artificial intelligence are better and achieve better results, both from a technical and economic point of view. The authors of [43] analyzed various off-grid renewable energy schemes for an informal settlement in Windhoek, Namibia. The study relied on HOMER Pro software for system sizing. It presented a technical and economic comparison between individual residential PV systems and powering the home via either a rooftop or ground-mounted hybrid microgrid from a roof-mounted or ground-mounted renewable energy system. In [44], a study was conducted to discuss the configuration of a hybrid system to feed some areas in India. Economic and technical aspects were studied. A combination of PVs, a WECS, a DG, and a BESS was used. The battery used was based on lead-acid flow technology. The residential community load was taken to obtain the best solutions.

Implementation of a hybrid home microgrid to supply an isolated home in a remote area was discussed in [45]. This hybrid microgrid combines PVs and a BESS. Optimization techniques were used for system sizing and energy management within the microgrid to reduce the total operating cost. This system succeeded in reducing operating costs by 23.13%. The system succeeded in reducing consumption by 18,161 kWh. Another study was conducted for power scheduling and energy management within a home microgrid in [46]. This microgrid was supported by vehicle-to-grid technology to satisfy the deficit during peak times. In [47], a power scheduling study was conducted in an isolated microgrid. The microgrid combined PVs and a WECS as the main sources. It was also supported by three backup sources, namely fuel cells, an electric vehicle, and a BESS. The system was supported by vehicle-to-grid technology. It succeeded in reducing the operating cost by 6.467%. Ref. [48] proposed a new deep-learning-based framework called Nemesyst depending on databases and model sequentialization. This framework is suitable for application to IoT aggregate control systems. It has been applied to demand-side response recommendations. In [49], an intelligent model for the effective scheduling control of smart networks depending on deep learning was presented. Another energy scheduling model based on the PSO was presented to achieve energy savings and reduce emissions as much as possible.

1.3. Contributions and Paper Organization

Many studies have discussed the sizing of microgrids, whether they were connected or isolated from the main grid. This paper proposes a detailed framework for electrifying a remote area in the Sahara Ténéré Desert of Niger. The paper presents some contributions that can be summarized as follows:

- A realistic power-scheduling approach is developed using highly dynamic meteorological and annual electric load data and the ability to operate the PV system in both off-grid and on-grid systems is proposed.
- A comprehensive analysis of the technical and economic performance of the three proposed cases is presented to illustrate the feasibility and productivity of the proposed techniques.
- Three cases of a microgrid configuration supplying a remote area in the Sahara Ténéré desert in northeastern Niger are presented and compared to choose the most cost-effective method, whether through an off-grid or on-grid system.
- An MILP-based framework is presented for optimal techno-economic power scheduling and sizing of the microgrid, considering stochasticity in the load demand.

This paper is divided into six sections. The first section discusses motivations, related works, and contributions. In Section 2, the problem description and proposed solutions, the nature of the site on which the study is being conducted, and the proposed microgrid system configurations and mathematical models of each component are discussed. The formulation including the objective function, constraints, and the MILP description are shown in Section 3. Section 4 describes the case study. The simulation results, analysis, and discussions are covered in Section 5. Finally, Section 6 gives the conclusions.

2. Methodology

2.1. Problem Description and Proposed Solutions

Many areas in African countries remain without access to electricity, or if they do have access, they still have a large deficit in this electricity. Niger is one of the countries that suffers with electricity poverty, especially in rural/isolated areas. Niger is a vast landlocked country in West Africa with a total land area of 1,267,000 km^2, as shown in Figure 1 (the dot marked on Niger's map indicates Niamey, which is the capital city). In the north, two-thirds of the country are covered by a dry tropical desert, i.e., the Sahara Desert. As of 2021, Niger's population was expected to be around 25 million people. Two seasons are observed throughout the year: the dry season lasting from October to May and the rainy season from June to September. Niger's average temperature lies between 21.9 °C and 36.4 °C. The country's electrification rate was only 15.78% (82.60% in urban areas and 1.21% in rural areas) in 2020.

Most of the remotely located populations are not connected to the grids, especially the Sahara Ténéré desert populations, who are located to almost 600 km away from the main electric grid in the north. Due to this factor, extending the grid to all dwellings and communities throughout Niger's Sahara Ténéré desert is difficult and economically unfeasible. All these communities are supplied by diesel generators, and are not covered by a 24-h power supply. It is not favorable to run these diesel generators because of the significant financial investment as well as the potentially hazardous environment they create. Hence, there is a need to diversify the sources of energy to ensure continuous and clean power supply, as well as minimal system costs, in these areas.

To overcome these problems, a techno-economic study of three cases was carried out to electrify a remote desert area located in the northeastern part of Niger, named Djado. The first and second cases are isolated systems. RESs are applied in the first case to cover the load entirely. In this case, the microgrid comprises a PV system and a battery bank energy storage system. A DG is added with PVs and a BESS in the second case. However, in the third case, the system is connected to the grid, where the grid participates in covering the load with PVs, the battery bank system, and a DG (used only in scenario 1 during the 2 h grid outage). A techno-economic study and analysis of these three cases were carried out to determine the best of them from an economic point of view to supply that remote desert

area. In this study, mixed-integer linear programming (MILP) was used as an optimization technique for the techno-economic analysis for optimal design selection.

Figure 1. Map of Africa showing Niger.

2.2. Site Description

Djado is the area under consideration. Djado is located about 900 km northeast of the Agadez region, Niger, in the Ténéré desert (Sahara), as shown in Figure 2. With the geographical location of 21°0′54″ north, 12°18′27″ east, Djado is the northernmost and easternmost town in Niger, bordered to the north by Algeria and Libya and to the east by Chad. The Djado area is well-known for its salt and date production. Its population was small until the discovery of Gold in April 2014, which caused several populations to move there in order to extract gold in traditional ways. This resulted in significant population growth among those who live without electricity. The climate in this region is variable throughout the year between hot and cold weather, but what distinguishes the region is that the weather conditions are very suitable for producing a sufficient amount of electrical energy from solar cells. Solar radiation is available throughout the year, about 317 sunny days per year, and is sufficient to produce a large amount of electricity.

Figure 2. Djado Plateau, Niger (21°00′54″ N, 12°18′27″ E).

2.3. Proposed Microgrid System Block Diagram Configurations and Mathematical Model

The schematic diagram of the microgrid system in three configurations, i.e., PV/battery bank, PV/battery bank/DG, and PV/battery bank/grid/DG (used only in scenario 1 during the 2 h grid outage), are given in Figure 3. This system was developed to satisfy the load demand of Djado, which remains without any means of electrical energy supply. The flowchart of each case's operating mechanism is presented in Figure 4.
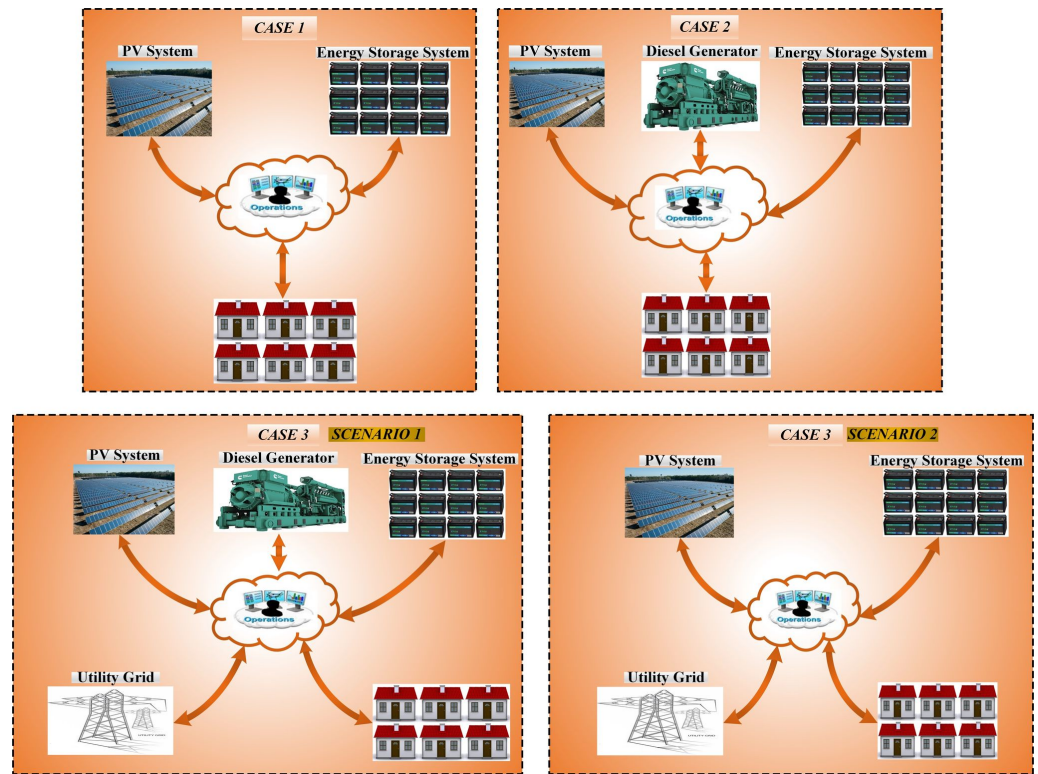

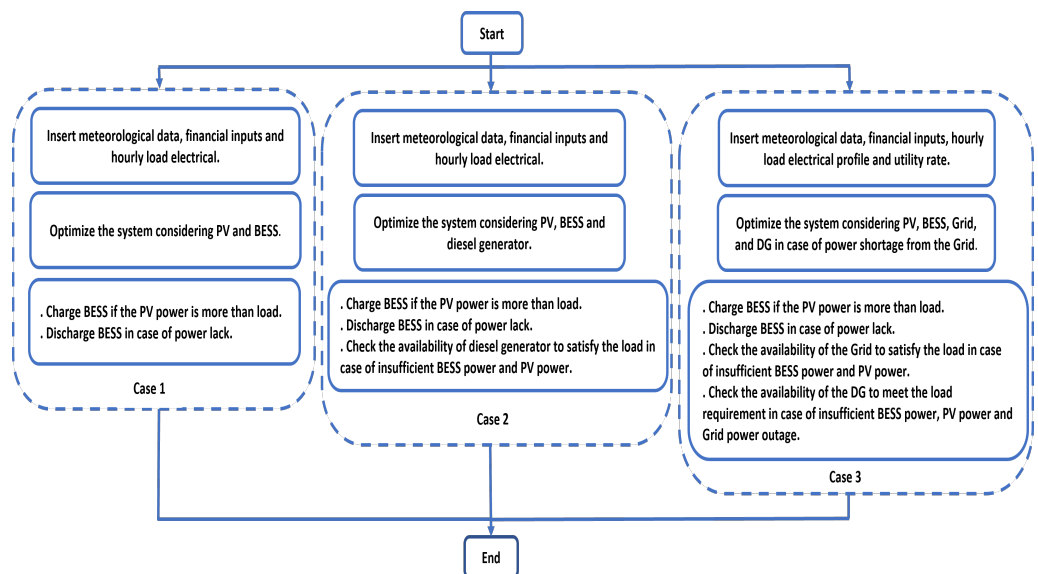**Figure 3.** Schematic diagram of the proposed microgrid in three cases.

Figure 4. Operating mechanism of each case study.

2.3.1. Modeling of Solar PV System

The use of solar energy has become increasingly popular in recent years. In PV systems, solar irradiation is converted into electricity directly without any environmental impact.

Solar cells are semiconductor p-n junctions and they constitute the main component of PV systems. A solar cell contains a photocurrent source, a single diode, and a resistor connected in parallel (R_{Sh}). In addition, there is a resistor connected in series (R_S), as shown in Figure 5.
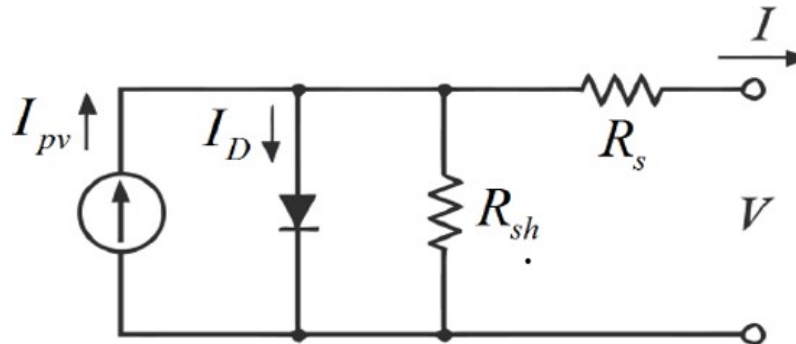

Figure 5. Equivalent circuit of a solar cell.

The mathematical model is represented as follows [45]:

$$I = I_{PV} - I_0 \left[\exp\left(\frac{V + IR_s}{\alpha V_T} \right) - 1 \right] - \left(\frac{V + IR_s}{R_{sh}} \right) \tag{1}$$

$$I_{PV} = (I_{PV-STC} + K_1 \Delta T) \frac{G}{G_{STC}} \tag{2}$$

$$I_o = I_{0-STC} \left(\frac{T_{STC}}{T} \right)^3 \exp\left[\frac{qE_g}{\alpha K} \left(\frac{1}{T_{STC}} - \frac{1}{T} \right) \right] \tag{3}$$

where Boltzmann's constant = 1.3805×10^{-23} J/K.

$$I = I_{PV} N_{sh} - I_o N_{sh} \left[\exp\left(\frac{V + IR_s \left(\frac{N_s}{N_{sh}} \right)}{\alpha V_T N_s} \right) - 1 \right] - \left(\frac{V + IR_s \left(\frac{N_s}{N_{sh}} \right)}{R_{sh} \left(\frac{N_s}{N_{sh}} \right)} \right) \tag{4}$$

Unlike shunt resistance, the effectiveness of a cell is significantly affected by changes in series resistance. In contrast, the change in the value of the shunt resistance does not have a significant impact [50]. In the case of infinite shunt resistance, the equation would be formulated as follows:

$$I = I_{PV} N_{sh} - I_o N_{sh} \left[\exp\left(\frac{V + IR_s \left(\frac{N_s}{N_{sh}} \right)}{\alpha V_T N_s} \right) - 1 \right] \tag{5}$$

The power produced from the *PV* can be calculated as represented by the equation shown below:

$$P_{PV}(r) = \begin{cases} P_{RS} \left(\frac{r^2}{R_{SRS} R_{CR}} \right) & 0 \le r < R_{CR} \\ P_{RS} \frac{r}{R_{SRS}} & R_{CR} \le r \le R_{SRS} \\ P_{RS} & R_{SRS} \le r \end{cases} \tag{6}$$

2.3.2. Modeling of Battery Energy Storage System

When using RESs in microgrids, the existence of an energy storage system is imperative and indispensable. The use of a BESS gives the electrical grid more reliability and effectiveness due to the intermittent and unstable nature of RESs. Batteries are connected in series and parallel to form the BESS. The battery capacity depends on many factors, such as the days of autonomy, which represent the number of days the battery will be capable of providing the energy required for the load without shortage. This is an essential factor that

should be considered when sizing batteries. The following formula can be used to calculate battery capacity [51]:

$$C_{batt} = \frac{AD \cdot P_{\text{L}}}{\eta_{\text{inv}} \cdot \eta_{Batt} \cdot DOD} \tag{7}$$

Depending on the state of charge (SOC), the battery can function as both a load and a source. It stores energy when there is a surplus in production while acting as a source and discharging to meet the energy deficit when there is a shortage of energy produced from RESs. Managing the charging and discharging processes is very important to maintain the battery's lifespan. The following equations represent the SOC of the battery during the charge and discharge process [11]:

- Charging process:

$$\text{SOC}(t+1) = (\text{SOC}(t) \cdot (1 - \sigma)) + ((E_{\text{gen},T}(t) - E_D(t)) \cdot \eta_{ch} \cdot \eta_{\text{rec}}) \tag{8}$$

- Discharging process:

$$\text{SOC}(t+1) = (\text{SOC}(t) \cdot (1 - \sigma)) - \left[\frac{E_D(t) - E_{\text{gen},T}(t)}{\eta_{\text{dch}} \cdot \eta_{\text{inv}}} \right] \tag{9}$$

2.3.3. Modeling of Diesel Generator (DG)

For hybrid systems, DGs are commonly used to provide power over periods of low irradiation and to feed the load demand at peak times, which can minimize the battery bank size in addition to the PV array size. To accomplish these tasks, the DG should have a good rating. To obtain the most suitable DG unit size, a detailed analysis is required of day-to-day and seasonal load fluctuations, growth in annual load, and consideration of practical constraints. In order to optimize fuel efficiency, a diesel cycling and dispatch strategy is often used with multiple units of various sizes to optimize the loading of the different units. The diesel generator fuel consumption, $Cons_D$ (L/h), depends on the output power and is defined by the following equation [52,53]:

$$Cons_D = B_D \cdot P_N^D + A_D \cdot P_D G \tag{10}$$

where B_D = 0.0845 (L/kWh) and A_D = 0.246 (L/kWh) are the coefficients of the consumption curve. The hourly cost of the fuel consumption can be expressed by Equation (11).

$$C_f = P_f uel \cdot Cons_D \tag{11}$$

The equation below expresses the performance of the DG [54].

$$\eta_{DG} = \frac{P_D G}{Cons_D \times LHV_f} \tag{12}$$

2.3.4. Grid Model

As mentioned previously, microgrids that rely solely on RESs suffer from unreliability and stability problems. Therefore, a BESS is relied upon, and in the event that it is unable to fill the deficit, the main grid is required to cover the energy shortage at peak times. In this case, the grid is relied upon as a backup source that sells electricity to the microgrid. The power supplied by the grid to the load can be expressed through the following equation:

$$P_{\text{grid}}(t) = P_{\text{L}}(t) - \sum (P_{PV}(t), P_{BESS}(t), P_{DG}(t)) \tag{13}$$

3. Formulation of the Optimization Problem

3.1. Objective Function

Total life cycle cost is an economic parameter set throughout the project's lifespan by considering the cost of all components. The life cycle cost of each component of the

hybrid microgrid system is the sum of investment, operation and maintenance costs, and replacement costs, minus salvage costs [55].

The life cycle cost of each component is given by [56]:

$$LCC = I_{invst} + C_{O\&M} + C_{\text{repl}} - C_{\text{salv}} \tag{14}$$

Initial investment cost encompasses the cost of purchasing and installing the system. Salvage cost is the earned cost at the end of the project's lifetime. The present value of the operating and maintenance cost is given by [57]:

$$\begin{cases} O\&M = (O\&M)_0 \times \frac{1+f}{1-f}\left(1 - \left(\frac{1+f}{1+i}\right)^n\right), & i \neq f \\ O\&M = (O\&M)_0 \times n, & i = f \end{cases} \tag{15}$$

In Niger, the inflation rate is 3.10% [58], while the interest rate is 4.75% [59].

In this paper, the total life cycle cost of the project is the objective function that is considered to be minimized. The objective function can be expressed as:

$$\min F = \min\left(\sum_{c=1}^{b}\left(I_{\text{invst}}(c) + C_{0\&M}(c) + C_{\text{repl}}(c) - C_{\text{salv}}(c)\right)\right) \tag{16}$$

3.2. Design Constraints

In microgrid hybrid systems, the power system components operate under constraints. The optimal operation of the system should satisfy the constraint function expressed in Equation (17), which means that the power is held in balance at any time.

The optimization approach is used to ensure that the hourly DG supplied power at any time is less than or equal to the DG rated power, as shown by Equation (20).

In order to avoid overcharging and deep discharging problems, the SOC of the battery bank is restrained and compared with the designed constraints at any hour during the operation period. Thus, the SOC of the battery storage system should fulfill the design constraints defined in Equations (21) and (22). $SOC_{\max}$, the maximum state of charge, is the full capacity of the battery bank, while $SOC_{\min}$, the minimum state of charge, depends mostly on the depth of discharge.

$$P_{PV}(t) + P_{DG}(t) + a \times P_{\text{BESS}}(t) = P_{\text{L}}(t) \tag{17}$$

$$a = \begin{cases} a = 1 \text{ discharge} \\ a = 0 \text{ charge stays constant} \\ a = -1 \text{ charge} \end{cases} \tag{18}$$

Under the main grid consideration, the equations below can be considered:

$$P_{\text{grid}}(t) + P_{PV}(t) + P_{DG}(t) + a \times P_{\text{BESS}}(t) = P_{\text{L}}(t) \tag{19}$$

$$P_{DG}(t) \leq P_{DG\_\text{rated}} \tag{20}$$

$$SOC_{\min} \leq SOC(t) \leq SOC_{\max} \tag{21}$$

$$SOC(t+1) = SOC(t)(1 - \sigma) \tag{22}$$

3.3. Mixed-Integer Linear Programming for the Microgrid Optimal Sizing

A mixed-integer linear programming (MILP) algorithm [60] is a solver for discrete optimization problems that uses many techniques to find the optimal solution from the objective function $f^T x$, where f is a linear function vector in which its elements are constant, and x is the solution vector. Bounds and linear constraints are the conditions of the MILP, but it has no nonlinear constraints. In particular, there are restrictions on the variables x

to be the integer. For a given objective function f, inequality matrices A_{ineq} and equality matrices A_{eq}, inequality vector b_{ineq} and equality vector b_{eq}, lower-bound l_b and upper-bound u_b, and the integer constraint "*intcon*", the problem model for finding a solution vector x from the feasible solution space is shown below:

$$\min_{x} f^T x$$

$$\text{subject to} \begin{cases} x(\text{intcon}) \text{ are integers} \\ A_{\text{ineq}} \cdot x \leq b_{\text{ineq}} \\ A_{eq} \cdot x = b_{eq} \\ l_b \leq x \leq u_b \end{cases} \tag{23}$$

The algorithm *intlinprog* uses six strategies to solve MILP and find the solution in any step. If it can find the solution in a step, *intlinprog* does not precede to the later step. The basic six strategies are shown as follows [60]:

- Reduce the problem size using linear program preprocessing;
- Solve an initial relaxed (non-integer) problem using linear programming;
- Perform mixed-integer program preprocessing to tighten the linear problem (LP) relaxation of the mixed-integer problem;
- Try to use the cutting-plane method to further tighten the LP relaxation of the mixed-integer problem as shown in Figure 6;
- Try to find integer-feasible solutions using heuristic;
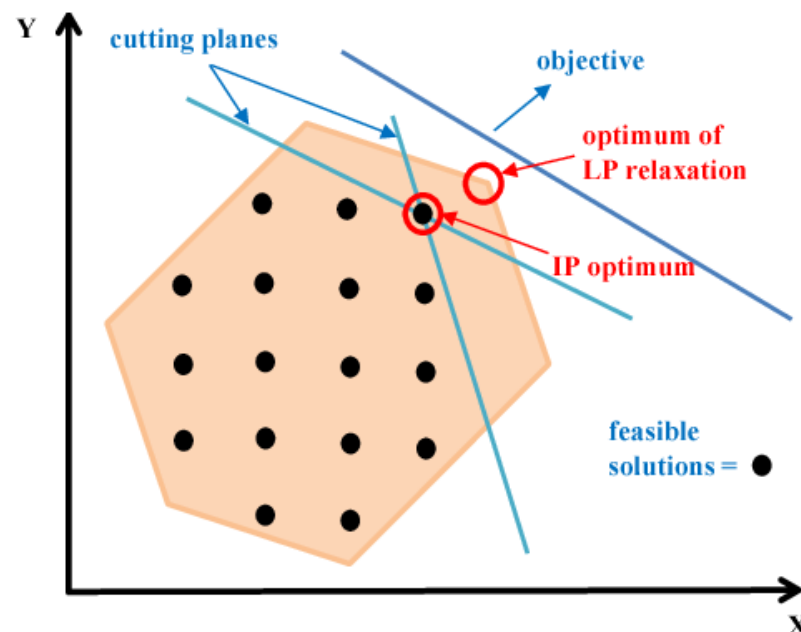- Use a branch and bound algorithm to search systematically for the optimum solution.

Figure 6. Cutting-plane method.

4. Case Study

The proposed methodology was used to find the optimal configuration of a hybrid microgrid system for an area located in Djado Plateau (21°0′54″ N, 12°18′27″ E), Niger, and analyze the results. This methodology is proposed to supply the residential households in that area. Three cases will be presented. In the first case, the microgrid system supplies the residential area through PVs and a BESS, while in the second case the load is supplied through PVs, a BESS, and a DG. In case 3, the grid participates in covering the load in

addition to PVs, a BESS, and a DG (used only in scenario 1 during the 2 h grid outage). The parameters of the microgrid components are represented in Table 1. The optimal sizing of the microgrid is implemented using MILP. The yearly load profile can be seen in Figure 7. In this region, the year is divided into two seasons: the dry season lasting from October to May and the rainy season from June to September. According to the load profile typically found in the remote Saharan areas of Niger, the hourly energy distributions are almost the same every day for each season. Therefore, the results will be presented for one week of each season.

Table 1. Parameters of the microgrid components.

| Component	Parameters	Value
PV	System capital cost ($/kW-DC)	500.00
	O&M cost ($/kW-DC per year)	2.0
	Array type	Ground mount, fixed
	Federal percentage-based incentive (%)	26
BESS	Energy capacity cost ($/kWh)	200.00
	Power capacity cost ($/kW)	400.00
	Energy capacity replacement cost ($/kWh)	180.00
	Inverter efficiency (%)	96
	Inverter replacement year	10
	Battery replacement year	10
	Minimum state of charge (%)	20
	Power capacity replacement cost ($/kW)	350.00
Diesel generator	Install cost ($/kW AC)	350.00
	Fixed O&M cost ($/kW per year)	5.00
	Diesel cost ($/gal)	1.00
	Generator replacement year	10
	Generator fuel cost escalation rate, nominal (%)	2.7
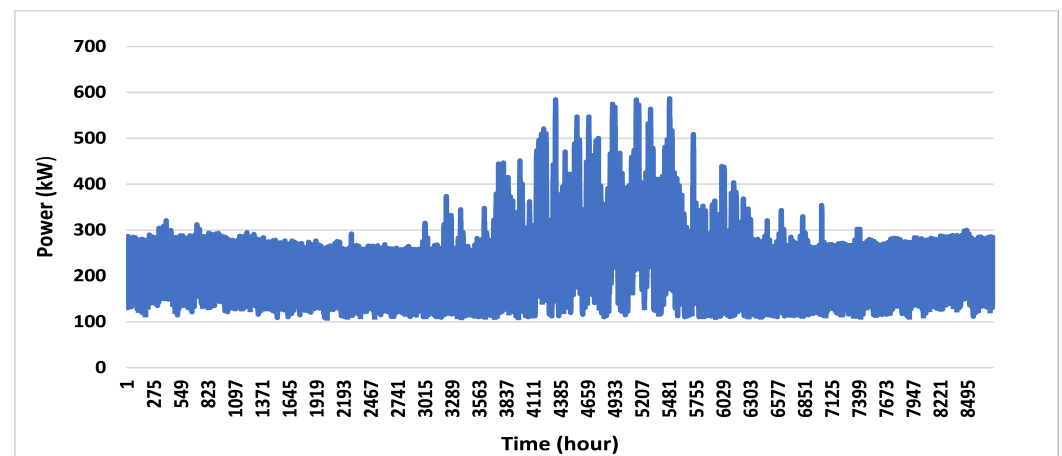
Figure 7. Hourly load profile during a year.

5. Optimization Results and Discussion

Several hybrid designs have been optimized in order to determine the most cost-efficient and power-balanced system. The results of three configurations will be evaluated and analyzed in this section.

5.1. Case 1

In this case, the PV system is relied upon to supply the residential loads. The BESS is used to increase the microgrid's reliability and overcome the intermittent nature of RESs, specifically PVs, which are used in this study because of the availability of solar radiation.

The suitable size of the PV system used in this case to cover the load is about 3180 kW, with a battery bank having a capacity of 5884 kWh. This configuration's total life-cycle cost is approximately $2,660,793, while the levelized cost of electricity is about 0.115 $/kWh. The annual average PV energy production is about 4,690,854 kWh. The annual operating and maintenance cost reached $6359. As mentioned earlier, there are two seasons in this region, i.e., dry and rainy (very short, not more than a month in a total of three months). Both seasons are regarded as hot seasons.

Figure 8 shows the results obtained for a week during the dry season in January, where the maximum electric load reached about 286.3 kW. Solar energy, by nature, is intermittent and not available throughout the day, so when there is a surplus, it is directed to charge the battery bank. The maximum value that the PVs achieved in serving the load was about 225.7 kW, while the maximum value directed to charging the battery bank was about 554.3 kW. The energy required to charge the batteries is later used to provide power to the loads when solar irradiation is unavailable. The highest discharge value in which the battery bank covered the load was about 286.3 kW. The SOC of the battery during this week is shown in Figure 9. The minimum SOC of the battery reached during this week was about 40%.
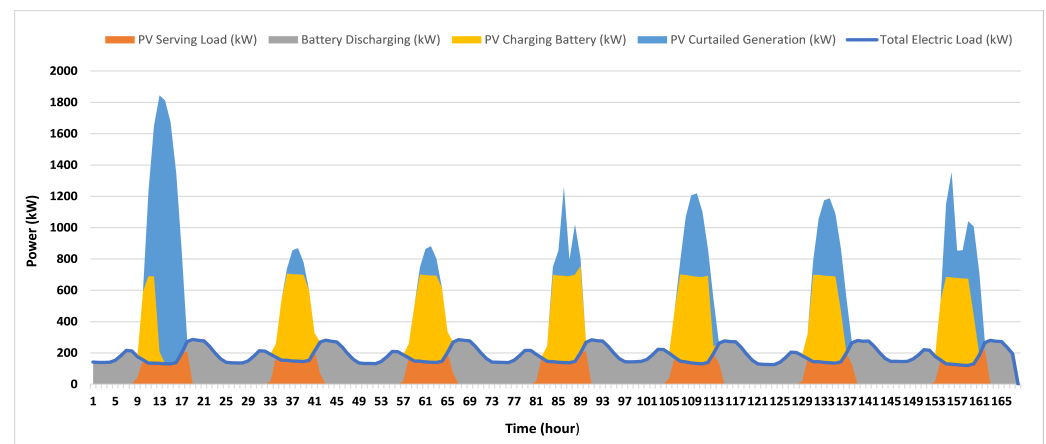

Figure 8. Microgrid operation during a week in the dry season: Case 1.
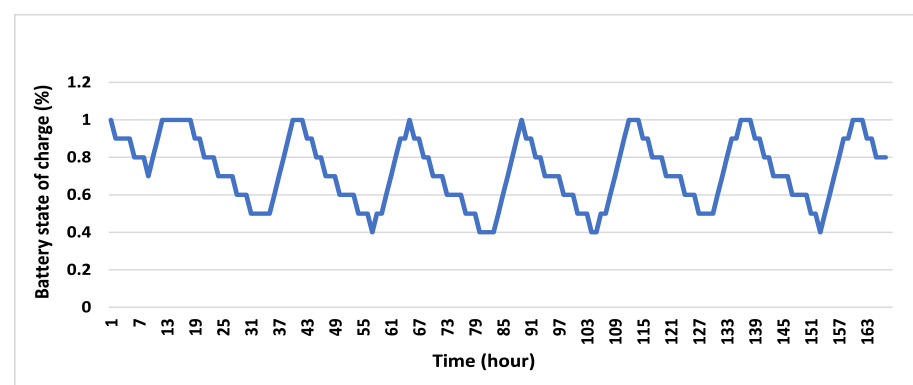

Figure 9. Battery state of charge during a week in the dry season: Case 1.

In the rainy (also hot) season, the electrical loads rise significantly, as shown in Figure 7. Since the results for a year cannot be presented in one figure, in addition to the need to show the difference in the generated power between the two seasons, the results for another week in the rainy season are presented. The load demand and the supplied energy during the selected week are shown in Figure 10. Electrical loads increase significantly, as shown in the considered week. The electrical load's highest value reached during this week was about 546.8 kW. This area is characterized by its high solar radiation, ideal for producing a

large amount of electrical energy. The PV system covers the loads during the day at times when solar radiation is available. The highest load covered by the PV was approximately 546.8 kW. The maximum value of power that the solar PV system supplied to charge the battery bank was 554.3 kW. The battery bank occasionally discharges to cover the demand when the PV power is insufficient. The highest discharged value from the battery bank was about 479.9 kW. The SOC of the battery during this week is shown in Figure 11.
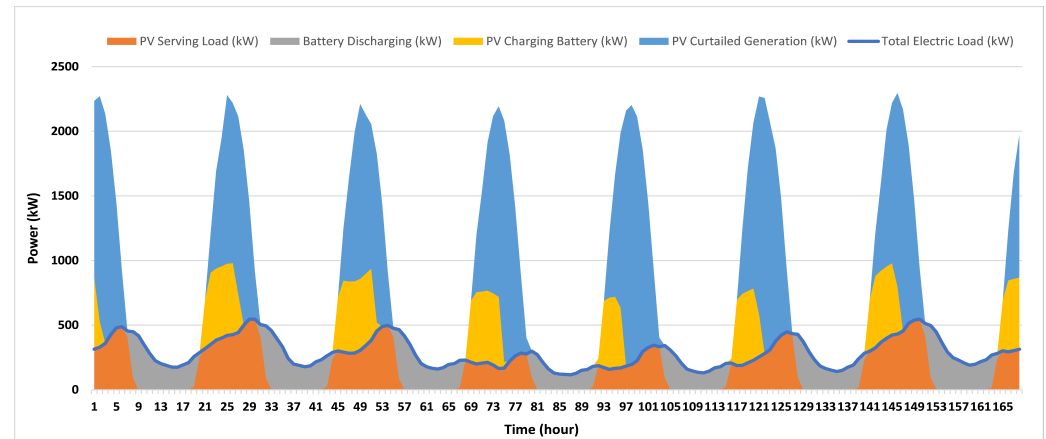

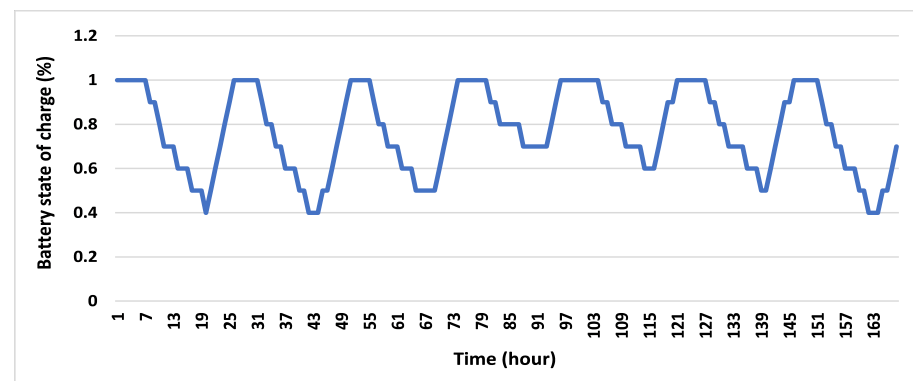**Figure 10.** Microgrid operation during a week in the rainy season: Case 1.

Figure 11. Battery state of charge during a week in the rainy season: Case 1.

5.2. Case 2

In this case, not only are the PV system and BESS relied upon to cover the residential loads, but DGs are used to cover the loads. It is estimated that the size of the PV system used is approximately 635 kW, with a battery bank capacity of 436 kWh. The generator size is 1174 kW.

In this configuration, the total life cycle cost is approximately $2,362,997, while the levelized cost of electricity is about 0.102 $/kWh. On average, per year, 937,356 kWh is the energy produced by the PV system. Approximately $7140 will be spent on operating and maintenance costs. The annual average DG production was found to be about 1,097,602 kWh, while the yearly diesel fuel used is about 83,418 gallons. PVs and the BESS will cover about 38% of the electrical load.

The power generated and loads for a week in the dry season are depicted in Figure 12. The peak load during that week is 286.3 kW. The highest power for which the PV system participated in covering the load was about 168.9 kW, while the one for which the PV system helped in charging the BESS was 142.9 kW. The BESS participated in covering the load at the times when it was difficult to use PVs and DGs. The source that is reliable for supplying the demand is chosen according to source availability and costs. The BESS took

part in covering the load with a capacity of 130.3 kW. Figure 13 presents the SOC for the considered week during the dry season.
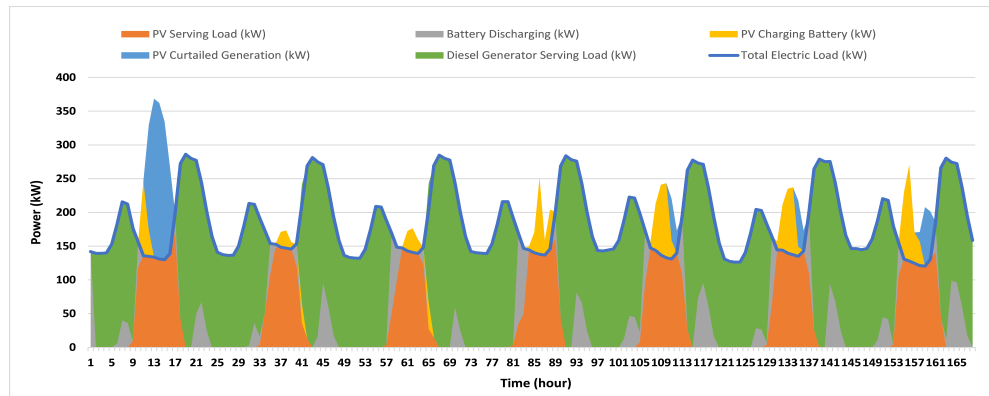

Figure 12. Microgrid operation during a week in the dry season: Case 2.
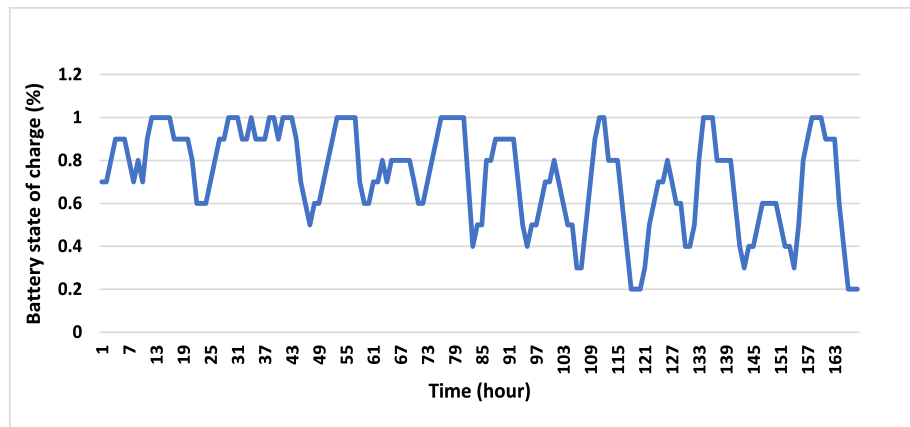

Figure 13. Battery state of charge during a week in the dry season: Case 2.

The results for a chosen week taken in the rainy season, also known as the hot season, are illustrated in Figure 14. The load demand increased significantly, and all three sources participated in covering it, taking into account the energy available from each source, the SOC of the battery, and the total cost. The PV supplied the load with 433.4 kW, while that which charged the BESS was 162.8 kW. However, the highest power values shared by the BESS and DG were about 131.2 kW and 448.5 kW, respectively. The SOC during this week is depicted in Figure 15. The minimum SOC of the battery during the week was 20%.
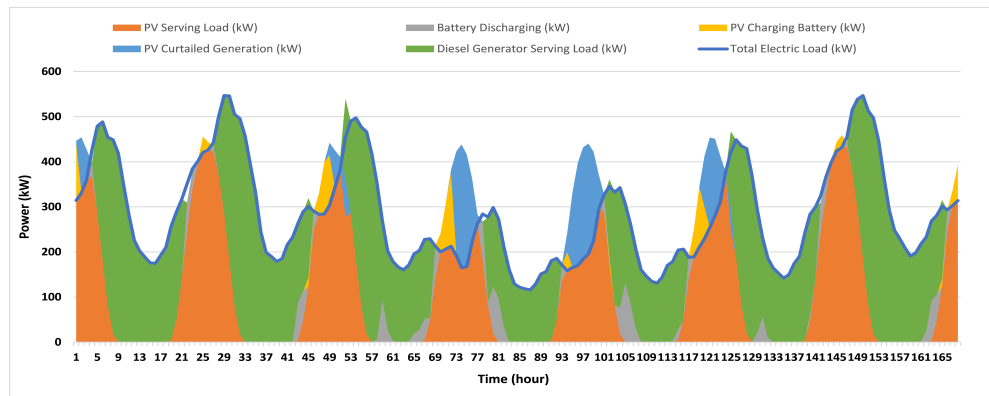

Figure 14. Microgrid operation during a week in the rainy season: Case 2.
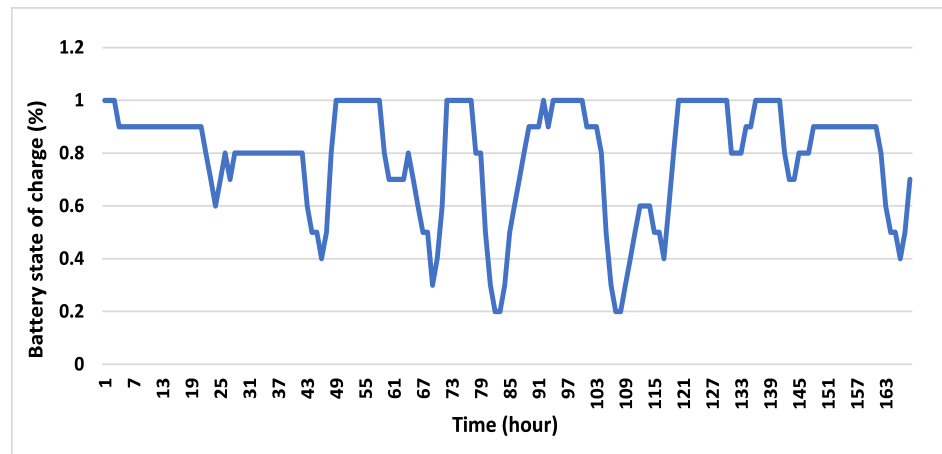
Figure 15. Battery state of charge during a week in the rainy season: Case 2.

5.3. *Case 3*

In this case, two scenarios were considered. In the first scenario, there was a power outage sometimes (about 2 h), and the DG was relied upon to cover this outage. In the second scenario, there was no power outage, and the DG was not used.

5.3.1. Scenario 1 (with power outage)

In this scenario, not only the PVs and BESS are required, but the grid participates in covering the load. To meet the load, a PV system with a capacity of 952 kW and a BESS with a capacity of 1045 kWh were utilized. A DG with a capacity of 1174 kW was used only for the 2 h shortage. It was estimated that the total life-cycle cost in this configuration was $2,504,862. The average annual PV energy production was about 1,403,952 kWh. The operating and maintenance costs that will be invested in this scenario are $7773.

In this scenario, the grid participates to a large extent in covering the load, as shown in Figure 16, which displays the results of a week in the dry season. The grid has served the load several times, and the highest value it supplied was 194.8 kW. In some periods, it did not participate because there was enough power generated from the PVs to supply the load. The highest value in which the PVs participated in supplying the load was 201.2 kW. The surplus was provided to charge the battery. The battery has partaken many times in feeding the load according to the SOC indicated in Figure 17.
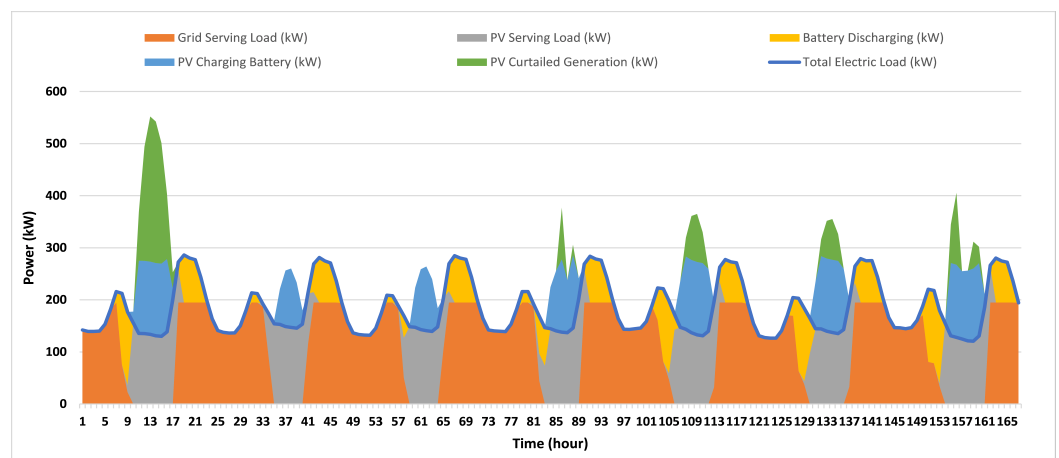

Figure 16. Microgrid operation during a week in the dry season: Case 3, Scenario 1.
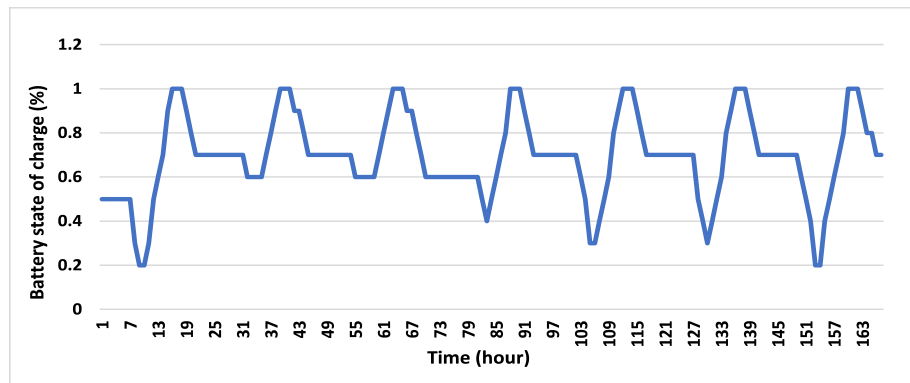
Figure 17. Battery state of charge during a week in the dry season: Case 3, Scenario 1.

The results obtained for a week in the rainy season are displayed in Figure 18. The grid participates in meeting the load significantly, with a higher load in this season. Figure 19 portrays the SOC of the BESS. The highest load detected during this week was 546.8 kW. The values of battery, grid, and PV participation in load coverage are 139.7 kW, 372.3 kW, and 515 kW, respectively.

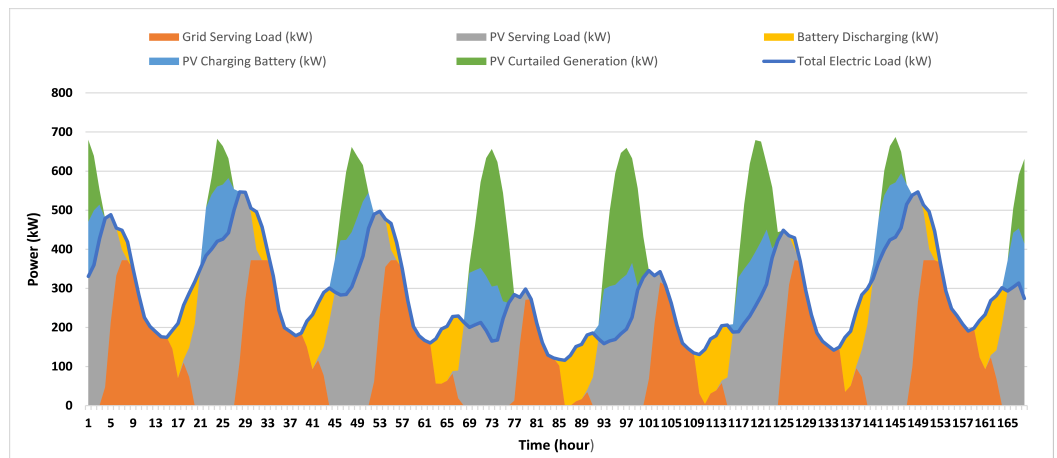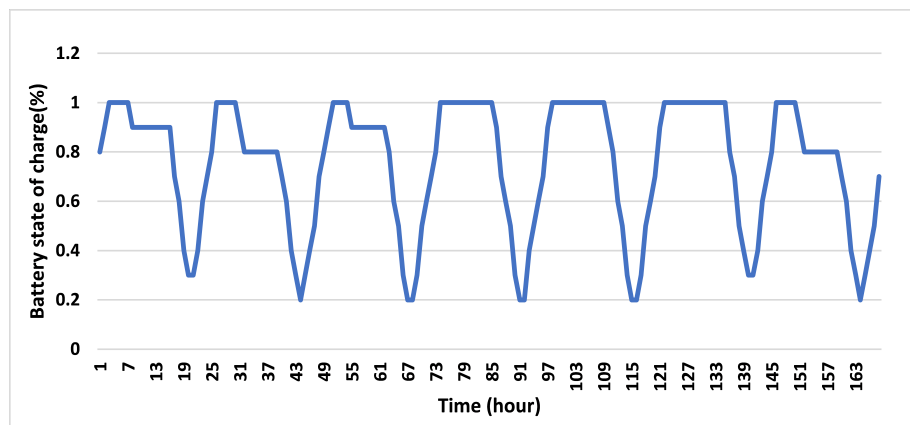**Figure 18.** Microgrid operation during a week in the rainy season: Case 3, Scenario 1.

Figure 19. Battery state of charge during a week in the rainy season: Case 3, Scenario 1.

The power outage occurred for two hours only during the year in this scenario. The outage began at 4 pm on 17 August and lasted for two hours. At that time, the DG covered the power shortage by contributing about 183 kW.

5.3.2. Scenario 2 (without Power Outage)

In this scenario, the DG is not called upon because no power outage occurred. The grid supports both the PVs and the BESS in making the balance with the load demand. The capacities of the PV system and the BESS were 954 kW and 1052 kWh, respectively.

This configuration was evaluated to have a total life-cycle cost of approximately $2,020,446. The average annual PV energy generation was 1,407,990 kWh and the annual operating and maintenance costs were $1909.

5.4. Economic Results Analysis and Discussion

This section analyzes and discusses the results of the three cases. Table 2 demonstrates a comparative summary of the three proposed cases.

In the first case, the PV array and the battery bank were the only generating sources. Therefore, the PV size and battery capacity were significantly larger in this case than in the other two cases, while the size of the PV was the lowest in the second case, and also the lowest battery size was observed in the third case. As a result, the total life-cycle cost in the first case was higher than the other cases, reaching $2,660,793, while it was the lowest value in the third case, i.e., scenario 2, at $2,020,446. The operating and maintenance costs were the lowest value in case 3, scenario 2, reaching $1909, whereas $7773 was the highest value in scenario 1 of the same case. The highest value, 4,690,854 kWh, was delivered by the PV system in case 1, while in case 2, it reached 937,356 kWh. Renewable electricity participation in meeting the demand reached 100%, 38%, and 54%, respectively, in cases 1, 2, and 3.

According to the obtained results, it is clear that the third case, scenario 2, is the most cost-effective, but it is difficult to implement due to the nature of the site on which the study was conducted. This case depends mainly on the grid; the studied area is remote and difficult to connect to the main grid because of the long separation distance of more than 600 km. Consequently, the second case is preferred due to not relying on the grid and achieving a small LCC.

Table 2. Comparison between the three operating cases.

Parameter	Case 1	Case 2	Case 3	
			Scenario 1	Scenario 2
Annual Site Load (kWh)	1,739,590	1,739,590	1,739,590	1,739,590
PV size (kW)	3180	635	952	954
Average Annual PV Energy Production (kWh)	4,690,854	937,356	1,403,952	1,407,990
Battery Bank Power (kW)	554	163	140	141
Battery Bank Capacity (kWh)	5884	436	1045	1052
Diesel Generator size (kW)	0	1174	1174	0
Total Life Cycle Cost ($)	2,660,793	2,362,997	2,504,862	2,020,446
Levelized Cost of Electricity ($/kWh)	0.115	0.102	0.13	0.13
Year 1 O&M costs ($) Before Tax	6359	7140	7773	1909
Annual Renewable Electricity (electricity consumption) (%)	100	38	54	54
Average Annual Energy Supplied from Grid (kWh)	0	0	794,598	794,628
Total Utility Electricity Cost ($)	0	0	1,253,311	1,251,771

6. Conclusions

Residential microgrids are primarily concerned with ensuring reliability and maximizing economic benefits. These are the two major concerns that must be considered when designing residential microgrids. In this paper we proposed three configurations for a cost-effective microgrid for a remote area in the Djado Plateau that lies in the Sahara Ténéré desert in northeastern Niger.

A comparative techno-economic analysis between three cases was presented and compared to determine the best configuration in terms of costs. The first case involved

PVs and a BESS, while the second case utilized PVs, a BESS, and a DG to supply the loads. PVs and a BESS collaborate with the grid to provide electricity to the load in the third case, which was subdivided into two scenarios: scenario 1 with a power outage, where a DG was used only for the two-hour shortage, and scenario 2 without a power outage. In order to reduce the cost of the microgrid , an optimal scheduling model was proposed. By analyzing the results for one year, MILP was used to determine the optimal sizing of the microgrid and grid power dispatch to reach the minimum LCC. The third case, scenario 2, had the least LCC, but it is difficult to implement because the study area is isolated and far from the main grid. The second case is preferred since it does not rely on grid power and achieves a small LCC, reaching about \$2,362,997 per year. It had a decrease in the value of the LCC by about 5.664% compared to the third case, scenario 1, while the decrease reached 11.19% compared to the first case. This demonstrates the effectiveness of using a system that combines PVs, a BESS, and a DG.

In future works, social, economic, and infrastructural aspects will be taken into account. A comprehensive analysis of these aspects will be conducted, and their impact will be studied in respect of the decision-making for grid extensions or relying entirely on RESs to provide electricity to households in remote rural/desert areas.

Nomenclature

The following abbreviations are used in this manuscript:

PV	Photovoltaic
BESS	Battery energy storage system
DG	Diesel generator
LCC	Life cycle cost
MILP	Mixed integer linear programming
WT	Wind turbine
WECS	Wind energy conversion system
HRES	Hybrid renewable energy system
HOMER	Hybrid optimization of multiple energy resources
GA	Genetic algorithm
TAC	Total annual cost
GOA	Grasshopper optimization algorithm
PSO	Particle swarm optimization
CS	Cuckoo search
DPSP	Deficiency of power supply probability
COE	Cost of energy
ABSO	Artificial bee swarm optimization
TS	Tabu search
SA	Simulated annealing
IPSO	Improved particle swarm optimization
IHS	Improved harmony search
IHSBSA	Improved-harmony-search-based simulated annealing
$LPSP_{max}$	Maximum loss of power supply probability
WOA	Whale optimization algorithm
WCA	Water cycle algorithm
MFO	Moth-flame optimizer
PSOGSA	Hybrid particle swarm-gravitational search algorithm

LPSP	Loss of power supply probability
NPC	Net present cost
NSGA	Non-dominated sorting genetic algorithm
RESs	Renewable energy sources
N	North
E	East
I	Supplied current to the load
I_{PV}	PV cell current
I_0	Reverse saturation current
V	Voltage across the diode
α	Ideality factor
V_T	Thermal voltage
R_S	Resistor connected in series
R_{Sh}	Resistor connected in parallel
I_{PV-STC}	Light generated current
K_1	Short circuit current temperature coefficient of the cell
ΔT	Temperature difference between the actual and nominal
G	Solar irradiation
G_{STC}	Nominal solar irradiation
I_{0-STC}	Nominal saturation current
T_{STC}	Temperature at standard test condition
T	Actual temperature
q	Charge of electrons
E_g	Energy band gap of semiconductor
N_s	Number of cells in series
N_{sh}	Number of cells in parallel
P_{RS}	PV panel rated power
r	Solar irradiation factor
R_{SRS}	Solar irradiation in standard environmental condition
R_{CR}	Certain radiation point set
C_{batt}	Battery capacity
AD	Days of autonomy
$P_{\text{L}}(t)$	Load demand at time t
η_{inv}	Inverter efficiency
η_{Batt}	Battery efficiency
DOD	Battery depth of discharge
$SOC(t)$	State of charge at time t
SOC_{mim}	Minimum state of charge
SOC_{max}	Maximum state of charge
σ	Hourly self-discharging rate
$E_{\text{gen},T}(t)$	Total energy generated at hour t
$E_D(t)$	Energy demand at hour t
η_{ch}	Charging efficiency
η_{dch}	Discharging efficiency
η_{rec}	Rectifier efficiency
η_{inv}	Inverter efficiency
P_N^D or $P_{DG-rated}$	Diesel generator rated power
$P_{DG(t)}$	Diesel generator output power at time t
C_f	Fuel consumption hourly cost
P_{fuel}	Fuel price
η_{DG}	DG performance
LHV_f	Fuel consumption heating value
$P_{\text{grid}}(t)$	Power supplied by the grid at time t
$P_{PV}(t)$	PV output power at time t
$P_{BESS}(t)$	BESS output power at time t
I_{invst}	Initial investment cost
$C_{O\&M}$	Operating and maintenance cost
C_{repl}	Replacement cost

C_{salv}	Salvage cost
O & M	Operating and maintenance
f	Inflation rate
i	Interest rate
n	Project lifespan
b	Number of components to be purchased related to the project

References

1. Lloyd, P.J. The role of energy in development. *J. Energy S. Afr.* **2017**, *28*, 54–62. [CrossRef]
2. Olatomiwa, L.; Mekhilef, S.; Ismail, M.S.; Moghavvemi, M. Energy management strategies in hybrid renewable energy systems: A review. *Renew. Sustain. Energy Rev.* **2016**, *62*, 821–835. [CrossRef]
3. Nguyen, K.H.; Kakinaka, M. Renewable energy consumption, carbon emissions, and development stages: Some evidence from panel cointegration analysis. *Renew. Energy* **2019**, *132*, 1049–1057. [CrossRef]
4. Ghorbani, B.; Mehrpooya, M.; Mousavi, S.A. Hybrid molten carbonate fuel cell power plant and multiple-effect desalination system. *J. Clean. Prod.* **2019**, *220*, 1039–1051. [CrossRef]
5. Hosseinalizadeh, R.; Shakouri, H.; Amalnick, M.S.; Taghipour, P. Economic sizing of a hybrid (PV–WT–FC) renewable energy system (HRES) for stand-alone usages by an optimization-simulation model: Case study of Iran. *Renew. Sustain. Energy Rev.* **2016**, *54*, 139–150. [CrossRef]
6. Zia, M.F.; Elbouchikhi, E.; Benbouzid, M. Microgrids energy management systems: A critical review on methods, solutions, and prospects. *Appl. Energy* **2018**, *222*, 1033–1055. [CrossRef]
7. Kumar, K.P.; Saravanan, B. Recent techniques to model uncertainties in power generation from renewable energy sources and loads in microgrids—A review. *Renew. Sustain. Energy Rev.* **2017**, *71*, 348–358. [CrossRef]
8. Elkadeem, M.; Wang, S.; Azmy, A.M.; Atiya, E.G.; Ullah, Z.; Sharshir, S.W. A systematic decision-making approach for planning and assessment of hybrid renewable energy-based microgrid with techno-economic optimization: A case study on an urban community in Egypt. *Sustain. Cities Soc.* **2020**, *54*, 102013. [CrossRef]
9. United Nations. Climate Action. Available online: https://www.un.org/en/climatechange/raising-ambition/renewable-energy (accessed on 28 June 2022).
10. Gao, K.; Wang, T.; Han, C.; Xie, J.; Ma, Y.; Peng, R. A review of optimization of microgrid operation. *Energies* **2021**, *14*, 2842. [CrossRef]
11. Elkholy, M.; Metwally, H.; Farahat, M.; Senjyu, T.; Lotfy, M.E. Smart centralized energy management system for autonomous microgrid using FPGA. *Appl. Energy* **2022**, *317*, 119164. [CrossRef]
12. Masrur, H.; Islam, M.R.; Muttaqi, K.M.; Gamil, M.M.; Huang, Y.; Senjyu, T. Resilience-aware optimal design and energy management scheme of multi-energy microgrids. In Proceedings of the 2021 IEEE Industry Applications Society Annual Meeting (IAS), Vancouver, BC, Canada, 10–14 October 2021; pp. 1–5.
13. Lian, J.; Zhang, Y.; Ma, C.; Yang, Y.; Chaima, E. A review on recent sizing methodologies of hybrid renewable energy systems. *Energy Convers. Manag.* **2019**, *199*, 112027. [CrossRef]
14. Dong, M.; Li, Y.; Song, D.; Yang, J.; Su, M.; Deng, X.; Huang, L.; Elkholy, M.; Joo, Y.H. Uncertainty and global sensitivity analysis of levelized cost of energy in wind power generation. *Energy Convers. Manag.* **2021**, *229*, 113781. [CrossRef]
15. Talaat, M.; Farahat, M.; Elkholy, M. Renewable power integration: Experimental and simulation study to investigate the ability of integrating wave, solar and wind energies. *Energy* **2019**, *170*, 668–682. [CrossRef]
16. Talaat, M.; Elkholy, M.; Farahat, M. Operating reserve investigation for the integration of wave, solar and wind energies. *Energy* **2020**, *197*, 117207. [CrossRef]
17. Talaat, M.; Elgarhy, A.; Elkholy, M.; Farahat, M. Integration of fuel cells into an off-grid hybrid system using wave and solar energy. *Int. J. Electr. Power Energy Syst.* **2021**, *130*, 106939. [CrossRef]
18. Alblawi, A.; Elkholy, M.; Talaat, M. ANN for assessment of energy consumption of 4 kW PV modules over a year considering the impacts of temperature and irradiance. *Sustainability* **2019**, *11*, 6802. [CrossRef]
19. Alblawi, A.; Said, T.; Talaat, M.; Elkholy, M. PV solar power forecasting based on hybrid MFFNN-ALO. In Proceedings of the 2022 13th International Conference on Electrical Engineering (ICEENG), Cairo, Egypt, 29–31 March 2022; pp. 52–56.
20. Talaat, M.; Elkholy, M.; Alblawi, A.; Said, T. Artificial intelligence applications for microgrids integration and management of hybrid renewable energy sources. *Artif. Intell. Rev.* **2023**, 1–55. [CrossRef]
21. Chambon, C.L.; Karia, T.; Sandwell, P.; Hallett, J.P. Techno-economic assessment of biomass gasification-based mini-grids for productive energy applications: The case of rural India. *Renew. Energy* **2020**, *154*, 432–444. [CrossRef]
22. Priyadharshini, B.; Ganapathy, V.; Sudhakara, P. An optimal model to meet the hourly peak demands of a specific region with solar, wind, and grid supplies. *IEEE Access* **2020**, *8*, 13179–13194. [CrossRef]
23. Gebrehiwot, K.; Mondal, M.A.H.; Ringler, C.; Gebremeskel, A.G. Optimization and cost-benefit assessment of hybrid power systems for off-grid rural electrification in Ethiopia. *Energy* **2019**, *177*, 234–246. [CrossRef]
24. Alturki, F.A.; Awwad, E.M. Sizing and cost minimization of standalone hybrid wt/pv/biomass/pump-hydro storage-based energy systems. *Energies* **2021**, *14*, 489. [CrossRef]

25. Veilleux, G.; Potisat, T.; Pezim, D.; Ribback, C.; Ling, J.; Krysztofiński, A.; Ahmed, A.; Papenheim, J.; Pineda, A.M.; Sembian, S.; et al. Techno-economic analysis of microgrid projects for rural electrification: A systematic approach to the redesign of Koh Jik off-grid case study. *Energy Sustain. Dev.* **2020**, *54*, 1–13. [CrossRef]

26. Odou, O.D.T.; Bhandari, R.; Adamou, R. Hybrid off-grid renewable power system for sustainable rural electrification in Benin. *Renew. Energy* **2020**, *145*, 1266–1279. [CrossRef]

27. Rullo, P.; Braccia, L.; Luppi, P.; Zumoffen, D.; Feroldi, D. Integration of sizing and energy management based on economic predictive control for standalone hybrid renewable energy systems. *Renew. Energy* **2019**, *140*, 436–451. [CrossRef]

28. Talaat, M.; Alblawi, A.; Tayseer, M.; Elkholy, M. FPGA control system technology for integrating the PV/wave/FC hybrid system using ANN optimized by MFO techniques. *Sustain. Cities Soc.* **2022**, *80*, 103825. [CrossRef]

29. Zhao, J.; Yuan, X. Multi-objective optimization of stand-alone hybrid PV-wind-diesel-battery system using improved fruit fly optimization algorithm. *Soft Comput.* **2016**, *20*, 2841–2853. [CrossRef]

30. Ma, T.; Yang, H.; Lu, L. A feasibility study of a stand-alone hybrid solar–wind–battery system for a remote island. *Appl. Energy* **2014**, *121*, 149–158. [CrossRef]

31. Belmili, H.; Haddadi, M.; Bacha, S.; Almi, M.F.; Bendib, B. Sizing stand-alone photovoltaic–wind hybrid system: Techno-economic analysis and optimization. *Renew. Sustain. Energy Rev.* **2014**, *30*, 821–832. [CrossRef]

32. Rehman, S.; Alam, M.M.; Meyer, J.P.; Al-Hadhrami, L.M. Feasibility study of a wind–pv–diesel hybrid power system for a village. *Renew. Energy* **2012**, *38*, 258–268. [CrossRef]

33. Rezzouk, H.; Mellit, A. Feasibility study and sensitivity analysis of a stand-alone photovoltaic–diesel–battery hybrid energy system in the north of Algeria. *Renew. Sustain. Energy Rev.* **2015**, *43*, 1134–1150. [CrossRef]

34. Rashid, F.; Hoque, M.E.; Aziz, M.; Sakib, T.N.; Islam, M.T.; Robin, R.M. Investigation of optimal hybrid energy systems using available energy sources in a rural area of Bangladesh. *Energies* **2021**, *14*, 5794. [CrossRef]

35. Hossain, M.S.; Jahid, A.; Islam, K.Z.; Rahman, M.F. Solar PV and biomass resources-based sustainable energy supply for off-grid cellular base stations. *IEEE Access* **2020**, *8*, 53817–53840. [CrossRef]

36. Bukar, A.L.; Tan, C.W.; Lau, K.Y. Optimal sizing of an autonomous photovoltaic/wind/battery/diesel generator microgrid using grasshopper optimization algorithm. *Sol. Energy* **2019**, *188*, 685–696. [CrossRef]

37. Maleki, A.; Pourfayaz, F. Optimal sizing of autonomous hybrid photovoltaic/wind/battery power system with LPSP technology by using evolutionary algorithms. *Sol. Energy* **2015**, *115*, 471–483. [CrossRef]

38. Zhao, B.; Zhang, X.; Li, P.; Wang, K.; Xue, M.; Wang, C. Optimal sizing, operating strategy and operational experience of a stand-alone microgrid on Dongfushan Island. *Appl. Energy* **2014**, *113*, 1656–1666. [CrossRef]

39. Diab, A.A.Z.; Sultan, H.M.; Mohamed, I.S.; Kuznetsov, O.N.; Do, T.D. Application of different optimization algorithms for optimal sizing of PV/wind/diesel/battery storage stand-alone hybrid microgrid. *IEEE Access* **2019**, *7*, 119223–119245. [CrossRef]

40. Islam, M.R.; Akter, H.; Howlader, H.O.R.; Senjyu, T. Optimal Sizing and Techno-Economic Analysis of Grid-Independent Hybrid Energy System for Sustained Rural Electrification in Developing Countries: A Case Study in Bangladesh. *Energies* **2022**, *15*, 6381. [CrossRef]

41. Ali, F.; Ahmar, M.; Jiang, Y.; AlAhmad, M. A techno-economic assessment of hybrid energy systems in rural Pakistan. *Energy* **2021**, *215*, 119103. [CrossRef]

42. Thirunavukkarasu, M.; Sawle, Y.; Lala, H. A comprehensive review on optimization of hybrid renewable energy systems using various optimization techniques. *Renew. Sustain. Energy Rev.* **2023**, *176*, 113192. [CrossRef]

43. Amupolo, A.; Nambundunga, S.; Chowdhury, D.S.; Grün, G. Techno-economic feasibility of off-grid renewable energy electrification schemes: A case study of an informal settlement in Namibia. *Energies* **2022**, *15*, 4235. [CrossRef]

44. Khan, F.A.; Pal, N.; Saeed, S.H.; Yadav, A. Techno-economic and feasibility assessment of standalone solar Photovoltaic/Wind hybrid energy system for various storage techniques and different rural locations in India. *Energy Convers. Manag.* **2022**, *270*, 116217. [CrossRef]

45. Elkholy, M.; Elymany, M.; Metwally, H.; Farahat, M.; Senjyu, T.; Lotfy, M.E. Design and implementation of a Real-time energy management system for an isolated Microgrid: Experimental validation. *Appl. Energy* **2022**, *327*, 120105. [CrossRef]

46. Elkholy, M.; Metwally, H.; Farahat, M.; Nasser, M.; Senjyu, T.; Lotfy, M.E. Dynamic centralized control and intelligent load management system of a remote residential building with V2H technology. *J. Energy Storage* **2022**, *52*, 104839. [CrossRef]

47. Elkholy, M.; Elymany, M.; Yona, A.; Senjyu, T.; Takahashi, H.; Lotfy, M.E. Experimental validation of an AI-embedded FPGA-based Real-Time smart energy management system using Multi-Objective Reptile search algorithm and gorilla troops optimizer. *Energy Convers. Manag.* **2023**, *282*, 116860. [CrossRef]

48. Onoufriou, G.; Bickerton, R.; Pearson, S.; Leontidis, G. Nemesyst: A hybrid parallelism deep learning-based framework applied for internet of things enabled food retailing refrigeration systems. *Comput. Ind.* **2019**, *113*, 103133. [CrossRef]

49. Tong, Z.; Zhou, Y.; Xu, K. An intelligent scheduling control method for smart grid based on deep learning. *Math. Biosci. Eng.* **2023**, *20*, 7679–7695. [CrossRef]

50. Elsonbaty, N.A.; Enany, M.A.; Gamil, M.M. Modelling of a directly coupled PV water pumping system using soft computing techniques. In Proceedings of the Michael Faraday IET International Summit 2015, Kolkata, India, 12–13 September 2015.

51. Fathy, A.; Kaaniche, K.; Alanazi, T.M. Recent approach based social spider optimizer for optimal sizing of hybrid PV/wind/battery/diesel integrated microgrid in Aljouf region. *IEEE Access* **2020**, *8*, 57630–57645. [CrossRef]

52. Yahiaoui, A.; Benmansour, K.; Tadjine, M. Control, analysis and optimization of hybrid PV-Diesel-Battery systems for isolated rural city in Algeria. *Sol. Energy* **2016**, *137*, 1–10. [CrossRef]
53. Ramli, M.A.; Hiendro, A.; Twaha, S. Economic analysis of PV/diesel hybrid system with flywheel energy storage. *Renew. Energy* **2015**, *78*, 398–405. [CrossRef]
54. Sari, A.; Majdi, A.; Opulencia, M.J.C.; Timoshin, A.; Huy, D.T.N.; Trung, N.D.; Alsaikhan, F.; Hammid, A.T.; Akhmedov, A. New optimized configuration for a hybrid PV/diesel/battery system based on coyote optimization algorithm: A case study for Hotan county. *Energy Rep.* **2022**, *8*, 15480–15492. [CrossRef]
55. Abbes, D.; Martinez, A.; Champenois, G. Life cycle cost, embodied energy and loss of power supply probability for the optimal design of hybrid power systems. *Math. Comput. Simul.* **2014**, *98*, 46–62. [CrossRef]
56. Kazem, H.A.; Albadi, M.; Al-Waeli, A.H.; Al-Busaidi, A.H.; Chaichan, M.T. Techno-economic feasibility analysis of 1 MW photovoltaic grid connected system in Oman. *Case Stud. Therm. Eng.* **2017**, *10*, 131–141. [CrossRef]
57. Kamjoo, A.; Maheri, A.; Dizqah, A.M.; Putrus, G.A. Multi-objective design under uncertainties of hybrid renewable energy system using NSGA-II and chance constrained programming. *Int. J. Electr. Power Energy Syst.* **2016**, *74*, 187–194. [CrossRef]
58. TRADING ECONOMICS. Available online: https://fr.tradingeconomics.com/niger/inflation-cpi (accessed on 28 January 2023).
59. TRADING ECONOMICS. Available online: https://tradingeconomics.com/niger/interest-rate (accessed on 28 January 2023).
60. Kuendee, P.; Janjarassuk, U. A comparative study of mixed-integer linear programming and genetic algorithms for solving binary problems. In Proceedings of the 2018 5th International Conference on Industrial Engineering and Applications (ICIEA), Singapore, 26–28 April 2018; pp. 284–288.